

An explicit unconditionally stable numerical method for solving damped nonlinear Schrödinger equations with a focusing nonlinearity

Weizhu Bao *

Department of Computational Science
National University of Singapore, Singapore 117543

Dieter Jaksch †

Institut für Theoretische Physik, Universität Innsbruck,
A-6020 Innsbruck, Austria.

Abstract

This paper introduces an extension of the time-splitting sine-spectral (TSSP) method for solving damped focusing nonlinear Schrödinger equations (NLS). The method is explicit, unconditionally stable and time transversal invariant. Moreover, it preserves the exact decay rate for the normalization of the wave function if linear damping terms are added to the NLS. Extensive numerical tests are presented for cubic focusing nonlinear Schrödinger equations in 2d with a linear, cubic or a quintic damping term. Our numerical results show that quintic or cubic damping always arrests blowup, while linear damping can arrest blowup only when the damping parameter δ is larger than a threshold value δ_{th} . We note that our method can also be applied to solve the 3d Gross-Pitaevskii equation with a quintic damping term to model the dynamics of a collapsing and exploding Bose-Einstein condensate (BEC).

Key Words. Damped nonlinear Schrödinger equation (DNLS); time-splitting sine-spectral method (TSSP), Gross-Pitaevskii equation (GPE), Bose-Einstein condensate (BEC), complex Ginzburg-Landau (CGL).

AMS subject classification. 35Q55, 65T40, 65N12, 65N35, 81-08

*Email address: bao@cz3.nus.edu.sg.

†Email address: dieter.jaksch@physics.oxford.ac.uk.

1 Introduction

Since the first experimental realization of Bose-Einstein condensation (BEC) in dilute weakly interacting gases the nonlinear Schrödinger equation (NLS) has been used extensively to describe the single particle properties of BECs. The results obtained by solving the NLS showed excellent agreement with most of the experiments (for a review see [4, 12, 11]). In fact, up to now there have been very few experiments in ultracold dilute bosonic gases which could not be described properly by using theoretical methods based on the NLS [22, 25].

Recent experiments by Donley *et al.* [13] provide new experimental results for checking the validity of describing a BEC by using the NLS in the case of attractive interactions (focusing nonlinearity) in 3d. Since the particle density might become very large in the case of attractive interactions inelastic collisions become important and cannot be neglected. These inelastic collisions are assumed to be accounted for by adding damping terms to the NLS. Two particle inelastic processes are taken into account by a cubic damping term while three particle inelastic collisions are described by a quintic damping term. Collisions with the background gas and feeding of the condensate can be studied by adding linear damping terms. One of the major theoretical challenges in comparing results obtained in the experiment with theoretical results is to find reliable methods for solving the NLS with a focusing nonlinearity and damping terms in the parameter regime where the experiments are performed.

The aim of this paper is to extend the time-splitting sine-spectral method (TSSP) for solving the focusing NLS with additional damping terms and to present extensive numerical tests. The comparison of our numerical results with the experimental results obtained for a collapsing BEC [13] will be presented elsewhere [9].

We consider the NLS [8, 38]

$$i \psi_t = -\frac{1}{2} \Delta \psi + V(\mathbf{x}) \psi - \beta |\psi|^{2\sigma} \psi, \quad t > 0, \quad \mathbf{x} \in \mathbb{R}^d, \quad (1.1)$$

$$\psi(\mathbf{x}, t = 0) = \psi_0(\mathbf{x}), \quad \mathbf{x} \in \mathbb{R}^d, \quad (1.2)$$

with $\sigma > 0$ a positive constant, where $\sigma = 1$ corresponds to a cubic nonlinearity and $\sigma = 2$ corresponds to a quintic nonlinearity, $V(\mathbf{x})$ is a real-valued potential whose shape is determined by the type of system under investigation, and β positive/negative corresponds to the focusing/defocusing NLS. In BEC, where (1.1) is also known as the Gross-Pitaevskii equation (GPE) [35], ψ is the macroscopic wave function of the condensate, t is time, \mathbf{x} is the spatial coordinate and $V(\mathbf{x})$ is a trapping potential which usually is harmonic and can thus be written as $V(\mathbf{x}) = \frac{1}{2} (\gamma_1^2 x_1^2 + \dots + \gamma_d^2 x_d^2)$ with $\gamma_1, \dots, \gamma_d \geq 0$. Two important invariants of (1.1) are the **normalization of the wave function**

$$N(t) = \int_{\mathbb{R}^d} |\psi(\mathbf{x}, t)|^2 d\mathbf{x}, \quad t \geq 0 \quad (1.3)$$

and the **energy**

$$E(t) = \int_{\mathbb{R}^d} \left[\frac{1}{2} |\nabla \psi(\mathbf{x}, t)|^2 + V(\mathbf{x}) |\psi(\mathbf{x}, t)|^2 - \frac{\beta}{\sigma + 1} |\psi(\mathbf{x}, t)|^{2\sigma+2} \right] d\mathbf{x}, \quad t \geq 0. \quad (1.4)$$

From the theory for the local existence of the solution of (1.1), it is well known that if $\|\psi(\cdot, t)\|_{H^1}$ is bounded, the solution exists for all t [38]. As a result, when the NLS is defocusing ($\beta < 0$), conservation of energy implies that $\int_{\mathbb{R}^d} |\nabla \psi(\mathbf{x}, t)|^2 d\mathbf{x}$ is bounded and the solution exists globally. On the other hand, if the NLS is focusing ($\beta > 0$) at critical ($\sigma d = 2$) or supercritical ($\sigma d > 2$) dimensions and for an initial energy $E(0) < 0$, the solutions of (1.1) can self-focus and become singular in finite time, i.e. there exists a time $t_* < \infty$ such that [38]

$$\lim_{t \rightarrow t_*} |\nabla \psi|_{L^2} = \infty \quad \text{and} \quad \lim_{t \rightarrow t_*} |\psi|_{L^\infty} = \infty.$$

However, the physical quantities modeled by ψ do not become infinite which implies that the validity of (1.1) breaks down near the singularity. Additional physical mechanisms, which were initially small, become important near the singular point and prevent the formation of the singularity. In BEC the particle density $|\psi|^2$ becomes large close to the critical point and inelastic collisions between particles which are negligible for small densities become important. Therefore a small damping (absorption) term is introduced into the NLS (1.1) which describes inelastic processes. We are interested in the cases where these damping mechanisms are important and, therefore, restrict ourselves to the case of focusing nonlinearities $\beta > 0$, where β may also be time dependent. We consider the following damped nonlinear Schrödinger equation:

$$i \psi_t = -\frac{1}{2} \Delta \psi + V(\mathbf{x}) \psi - \beta |\psi|^{2\sigma} \psi - i g(|\psi|^2) \psi, \quad t > 0, \quad \mathbf{x} \in \mathbb{R}^d, \quad (1.5)$$

$$\psi(\mathbf{x}, t = 0) = \psi_0(\mathbf{x}), \quad \mathbf{x} \in \mathbb{R}^d, \quad (1.6)$$

where $g(\rho) \geq 0$ for $\rho = |\psi|^2 \geq 0$ is a real-valued monotonically increasing function.

The general form of (1.5) covers many damped NLS arising in various different applications. In BEC, for example, when $g(\rho) \equiv 0$, (1.5) reduces to the usual GPE (1.1); a linear damping term $g(\rho) \equiv \delta$ with $\delta > 0$ describes inelastic collisions with the background gas; cubic damping $g(\rho) = \delta_1 \beta \rho$ with $\delta_1 > 0$ corresponds to two-body loss [37, 36]; and a quintic damping term of the form $g(\rho) = \delta_2 \beta^2 \rho^2$ with $\delta_2 > 0$ adds three-body loss to the GPE (1.1) [37, 36]. It's easy to see that the decay of the normalization according to (1.5) due to damping is given by

$$N'(t) = \frac{d}{dt} \int_{\mathbb{R}^d} |\psi(\mathbf{x}, t)|^2 d\mathbf{x} = -2 \int_{\mathbb{R}^d} g(|\psi(\mathbf{x}, t)|^2) |\psi(\mathbf{x}, t)|^2 d\mathbf{x} \leq 0, \quad t > 0. \quad (1.7)$$

Particularly, if $g(\rho) \equiv \delta$ with $\delta > 0$, the normalization is given by

$$N(t) = \int_{\mathbb{R}^d} |\psi(\mathbf{x}, t)|^2 d\mathbf{x} = e^{-2\delta t} N(0) = e^{-2\delta t} \int_{\mathbb{R}^d} |\psi_0(\mathbf{x})|^2 d\mathbf{x}, \quad t \geq 0. \quad (1.8)$$

There has been a series of recent studies which deals with the analysis and numerical solution of the damped NLS. Fibich [16] analyzed the effect of linear damping (absorption) on the critical self-focusing NLS, Tsutsumi [39, 40] studied the global solutions of the NLS with linear damping, the regularity of attractors and approximate inertial manifolds for a weakly damped NLS were given in Goubet [21, 20] and by Jolly *et al.* [26]. For numerically solving the linearly damped NLS Peranish [34] proposed a finite difference scheme and this method was revisited recently by Ciegis *et al.* [10] and Zhang *et al.* [41]. Moebs [32] presented a multilevel method for weakly damped NLS and applied it to solve a stochastic weakly damped NLS in [31]. Variable mesh difference schemes for the NLS with a linear damping term were used by Iyengar *et al.* [24].

Also the TSSP, which we will use in this paper to solve the damped NLS, was already successfully used for solving the Schrödinger equation in the semiclassical regime and for describing Bose-Einstein condensation using the Gross-Pitaeskkii equation by Bao *et al.* [5, 6, 8]. The TSSP is explicit, unconditionally stable and time transversal invariant. Moreover, it gives the exact decay rate of the normalization when linear damping is applied to the NLS (i.e. $g(\rho) \equiv \delta$ with $\delta > 0$ in (1.5)) and yields spectral accuracy for spatial derivatives and second-order accuracy for the time derivative. Thus this method is a very good candidate for solving the damped NLS, especially in 2d or 3d. We test the novel numerical method extensively in 2d.

Finally, we want to emphasize that the NLS is also used in nonlinear optics, e.g., to describe the propagation of an intense laser beam through a medium with a Kerr nonlinearity [18, 38]. In nonlinear optics $\psi = \psi(\mathbf{x}, t)$ describes the electrical field amplitude, t is the spatial coordinate in the direction of propagation, $\mathbf{x} = (x_1, \dots, x_d)^T$ is the transverse spatial coordinate and $V(\mathbf{x})$ is determined by the index of refraction. Nonlinear damping terms of the form $g(\rho) = \delta\beta^q\rho^q$ with $\delta, q > 0$ correspond to multiphoton absorption processes [16].

The paper is organized as follows. In section 2 we present the time-splitting sine-spectral approximation for the damped nonlinear Schrödinger equation. In section 3 numerical tests are presented for the cubic focusing nonlinear Schrödinger equation in 2d with a linear, cubic or quintic damping term. In section 4 some conclusions are drawn.

2 Time-splitting sine-spectral method

In this section we present a time-splitting sine-spectral (TSSP) method for solving the problem (1.5), (1.6) with homogeneous periodic boundary conditions. For simplicity of notation we shall introduce the method for the case of one spatial dimension ($d = 1$). Generalizations to $d > 1$ are straightforward for tensor product grids and the results remain valid without modifications. For $d = 1$, the problem becomes

$$i \psi_t = -\frac{1}{2}\psi_{xx} + V(x)\psi - \beta|\psi|^{2\sigma}\psi - i g(|\psi|^2)\psi, \quad a < x < b, \quad t > 0, \quad (2.1)$$

$$\psi(x, t = 0) = \psi_0(x), \quad a \leq x \leq b, \quad \psi(a, t) = \psi(b, t) = \mathbf{0}, \quad t \geq 0. \quad (2.2)$$

2.1 General damping term

We choose the spatial mesh size $h = \Delta x > 0$ with $h = (b - a)/M$ and M an even positive integer, the time step is given by $k = \Delta t > 0$ and define grid points and time steps by

$$x_j := a + j h, \quad t_n := n k, \quad j = 0, 1, \dots, M, \quad n = 0, 1, 2, \dots$$

Let ψ_j^n be the numerical approximation of $\psi(x_j, t_n)$ and ψ^n the solution vector at time $t = t_n = nk$ with components ψ_j^n .

From time $t = t_n$ to time $t = t_{n+1}$, the damped nonlinear Schrödinger equation (2.1) is solved in two steps. One solves

$$i \psi_t = -\frac{1}{2} \psi_{xx}, \quad (2.3)$$

for one time step, followed by solving

$$i \psi_t(x, t) = V(x)\psi(x, t) - \beta |\psi(x, t)|^{2\sigma} \psi(x, t) - i g(|\psi(x, t)|^2) \psi(x, t), \quad (2.4)$$

again for the same time step. Equation (2.3) is discretized in space by the sine-spectral method and integrated in time *exactly*. For $t \in [t_n, t_{n+1}]$, multiplying the ODE (2.4) by $\overline{\psi(x, t)}$, the conjugate of $\psi(x, t)$, one obtains

$$i \psi_t(x, t) \overline{\psi(x, t)} = V(x) |\psi(x, t)|^2 - \beta |\psi(x, t)|^{2\sigma+2} - i g(|\psi(x, t)|^2) |\psi(x, t)|^2. \quad (2.5)$$

Subtracting the conjugate of Eq. (2.5) from Eq. (2.5) and multiplying by $-i$ one obtains

$$\frac{d}{dt} |\psi(x, t)|^2 = \overline{\psi_t(x, t)} \psi(x, t) + \psi_t(x, t) \overline{\psi(x, t)} = -2g(|\psi(x, t)|^2) |\psi(x, t)|^2. \quad (2.6)$$

Let

$$f(s) = \int \frac{1}{s g(s)} ds, \quad h(s, \tau) = \begin{cases} f^{-1}(f(s) - 2\tau), & s > 0, \tau \geq 0, \\ 0, & s = 0, \tau \geq 0. \end{cases} \quad (2.7)$$

Then, if $g(s) \geq 0$ for $s \geq 0$, we find

$$0 \leq h(s, \tau) \leq s, \quad \text{for } s \geq 0, \tau \geq 0 \quad (2.8)$$

and the solution of the ODE (2.6) can be expressed as (with $\tau = t - t_n$)

$$\begin{aligned} 0 \leq \rho(t) &= \rho(t_n + \tau) := |\psi(x, t)|^2 = h(|\psi(x, t_n)|^2, t - t_n) := h(\rho(t_n), \tau) \\ &\leq \rho(t_n) = |\psi(x, t_n)|^2, \quad t_n \leq t \leq t_{n+1}. \end{aligned} \quad (2.9)$$

Combining Eq. (2.9) and Eq. (2.4) we obtain

$$i \psi_t(x, t) = V(x)\psi(x, t) - \beta \left[h \left(|\psi(x, t_n)|^2, t - t_n \right) \right]^\sigma \psi(x, t) - i g \left(h \left(|\psi(x, t_n)|^2, t - t_n \right) \right) \psi(x, t), \quad t_n \leq t \leq t_{n+1}. \quad (2.10)$$

Integrating (2.10) from t_n to t , we find

$$\psi(x, t) = \exp \left\{ i \left[-V(x)(t - t_n) + G \left(|\psi(x, t_n)|^2, t - t_n \right) \right] - F \left(|\psi(x, t_n)|^2, t - t_n \right) \right\} \times \psi(x, t_n), \quad t_n \leq t \leq t_{n+1}, \quad (2.11)$$

where we have defined

$$F(s, r) = \int_0^r g(h(s, \tau)) d\tau \geq 0, \quad G(s, r) = \int_0^r \beta [h(s, \tau)]^\sigma d\tau. \quad (2.12)$$

To find the time evolution between $t = t_n$ and $t = t_{n+1}$, we combine the splitting steps via the standard second-order Strang splitting (TSSP) for solving the damped nonlinear Schrödinger equation (2.1). In detail, the steps for obtaining ψ_j^{n+1} from ψ_j^n are given by

$$\begin{aligned} \psi_j^* &= \exp \left\{ -F \left(|\psi_j^n|^2, k/2 \right) + i \left[-V(x_j)k/2 + G \left(|\psi_j^n|^2, k/2 \right) \right] \right\} \psi_j^n, \\ \psi_j^{**} &= \sum_{l=1}^{M-1} e^{-ik\mu_l^2/2} \widehat{\psi}_l^* \sin(\mu_l(x_j - a)), \quad j = 1, 2, \dots, M-1, \\ \psi_j^{n+1} &= \exp \left\{ -F \left(|\psi_j^{**}|^2, k/2 \right) + i \left[-V(x_j)k/2 + G \left(|\psi_j^{**}|^2, k/2 \right) \right] \right\} \psi_j^{**}, \end{aligned} \quad (2.13)$$

where \widehat{U}_l are the sine-transform coefficients of a complex vector $U = (U_0, U_1, \dots, U_M)$ with $U_0 = U_M = \mathbf{0}$ which are defined as

$$\mu_l = \frac{\pi l}{b-a}, \quad \widehat{U}_l = \frac{2}{M} \sum_{j=1}^{M-1} U_j \sin(\mu_l(x_j - a)), \quad l = 1, 2, \dots, M-1, \quad (2.14)$$

where

$$\psi_j^0 = \psi(x_j, 0) = \psi_0(x_j), \quad j = 0, 1, 2, \dots, M. \quad (2.15)$$

Note that the only time discretization error of TSSP is the splitting error, which is second order in k if the integrals in (2.7) and (2.12) can be evaluated analytically.

2.2 Most frequently used damping terms

In this subsection we present explicit formulae for using TSSP when solving the NLS with those damping terms most frequently appearing in BEC and nonlinear optics.

Case I NLS with a linear damping term. We choose $g(\rho) \equiv \delta$ with $\delta > 0$ in (1.5). In BEC this damping terms describes inelastic collisions of condensate particles with the background gas. From (2.7), we find

$$f(s) = \int \frac{1}{\delta s} ds = \frac{1}{\delta} \ln s \quad \text{and} \quad h(s, \tau) = e^{-2\delta\tau} s. \quad (2.16)$$

Substituting (2.16) into (2.9) and (2.12), we obtain

$$\rho(t) = e^{-2\delta(t-t_n)} |\psi(x, t_n)|^2, \quad t_n \leq t \leq t_{n+1}, \quad (2.17)$$

$$F(s, r) = \delta r, \quad (2.18)$$

$$G(s, r) = \frac{\beta s^\sigma}{2\delta\sigma} (1 - e^{-2\delta\sigma r}). \quad (2.19)$$

Substituting (2.18) and (2.19) into (2.13), we get the following second-order time-splitting sine-spectral steps for the NLS with a linear damping term

$$\begin{aligned} \psi_j^* &= \exp \left\{ -k\delta/2 + i \left[-V(x_j)k/2 + \beta |\psi_j^n|^{2\sigma} (1 - e^{-\delta\sigma k}) / (2\delta\sigma) \right] \right\} \psi_j^n, \\ \psi_j^{**} &= \sum_{l=1}^{M-1} e^{-ik\mu_l^2/2} \widehat{\psi}_l^* \sin(\mu_l(x_j - a)), \quad j = 1, 2, \dots, M-1, \\ \psi_j^{n+1} &= \exp \left\{ -k\delta/2 + i \left[-V(x_j)k/2 + \beta |\psi_j^{**}|^{2\sigma} (1 - e^{-\delta\sigma k}) / (2\delta\sigma) \right] \right\} \psi_j^{**}. \end{aligned} \quad (2.20)$$

Case II NLS with a damping term of the form $g(\rho) = \delta\beta^q\rho^q$, where $\delta, q > 0$ in (1.5). For $q = 1$ ($q = 2$) we obtain the damping term describing two (three) particle inelastic collisions in BEC. From (2.7) we get

$$f(s) = \int \frac{1}{\delta\beta^q s^{q+1}} ds = -\frac{1}{q\delta\beta^q s^q} \quad \text{and} \quad h(s, \tau) = \frac{s}{(1 + 2q\delta\tau\beta^q s^q)^{1/q}}. \quad (2.21)$$

Substituting (2.21) into (2.9) and (2.12), we obtain

$$\rho(t) = \frac{|\psi(x, t_n)|^2}{[1 + 2q\delta\beta^q(t - t_n)|\psi(x, t_n)|^{2q}]^{1/q}}, \quad t_n \leq t \leq t_{n+1}, \quad (2.22)$$

$$F(s, r) = \frac{1}{2q} \ln(1 + 2q\delta r\beta^q s^q), \quad (2.23)$$

$$G(s, r) = \begin{cases} \frac{\beta^{1-q}}{2\delta q} \ln(1 + 2q\delta r\beta^q s^q) & q = \sigma, \\ \frac{\beta^{1-q} s^{\sigma-q} [-1 + (1 + 2q\delta r\beta^q s^q)^{(q-\sigma)/q}]}{2\delta(q-\sigma)} & \sigma \neq q. \end{cases} \quad (2.24)$$

Substituting (2.23) and (2.24) into (2.13), we get the following second-order time-splitting sine-spectral method for the NLS

$$\begin{aligned} \psi_j^* &= \begin{cases} \frac{\exp \left\{ i \left[-V(x_j)k/2 + \beta^{1-q} \ln(1 + \delta q k \beta^q |\psi_j^n|^{2q}) / (2\delta q) \right] \right\}}{(1 + q\delta k \beta^q |\psi_j^n|^{2q})^{1/2q}} \psi_j^n, & \sigma = q, \\ \frac{\exp \left\{ i \left[-\frac{V(x_j)k}{2} + \frac{\beta^{1-q} |\psi_j^n|^{2\sigma-2q}}{2\delta(q-\sigma)} \left(-1 + (1 + \delta q k \beta^q |\psi_j^n|^{2q})^{\frac{q-\sigma}{q}} \right) \right] \right\}}{(1 + q\delta k \beta^q |\psi_j^n|^{2q})^{1/2q}} \psi_j^n, & \sigma \neq q, \end{cases} \\ \psi_j^{**} &= \sum_{l=1}^{M-1} e^{-ik\mu_l^2/2} \widehat{\psi}_l^* \sin(\mu_l(x_j - a)), \quad j = 1, 2, \dots, M-1, \end{aligned} \quad (2.25)$$

$$\psi_j^{n+1} = \begin{cases} \frac{\exp \left\{ i \left[-V(x_j)k/2 + \beta^{1-q} \ln \left(1 + \delta q k \beta^q |\psi_j^{**}|^{2q} \right) / (2\delta q) \right] \right\}}{(1 + q\delta k \beta^q |\psi_j^{**}|^{2q})^{1/2q}} \psi_j^{**}, & \sigma = q, \\ \frac{\exp \left\{ i \left[-\frac{V(x_j)k}{2} + \frac{\beta^{1-q} |\psi_j^{**}|^{2\sigma-2q}}{2\delta(q-\sigma)} \left(-1 + (1 + \delta q k \beta^q |\psi_j^{**}|^{2q})^{\frac{q-\sigma}{q}} \right) \right] \right\}}{(1 + q\delta k \beta^q |\psi_j^{**}|^{2q})^{1/2q}} \psi_j^{**}, & \sigma \neq q. \end{cases}$$

Case III Focusing cubic NLS with a damping term that accounts for two-body and three-body loss in a BEC [37], i.e., we choose $\sigma = 1$, $g(\rho) = \delta_1 \beta \rho + \delta_2 \beta^2 \rho^2$ with $\delta_1, \delta_2 > 0$, in (1.5). Using (2.7), we get

$$f(s) = \begin{cases} -\frac{1}{\delta_1 \beta s} + \frac{\delta_2}{\delta_1} \ln(\delta_2 \beta + \delta_1/s), & s > 0, \\ 0, & s = 0. \end{cases} \quad (2.26)$$

Substituting (2.7) into (2.12) and changing the variable of integration we obtain

$$\begin{aligned} F(s, r) &= \int_0^r g(f^{-1}(f(s) - 2\tau)) d\tau \stackrel{\tau=(f(s)-f(h))/2}{=} \int_s^{h(s,r)} -\frac{1}{2} g(h) f'(h) dh \\ &= \int_s^{h(s,r)} -\frac{1}{2h} dh = \begin{cases} -\frac{1}{2} \ln(h(s, r)/s), & s > 0, \\ 0 & s = 0; \end{cases} \end{aligned} \quad (2.27)$$

where $h(s, r)$ is the solution of

$$f(s) - f(h(s, r)) = 2r, \quad \text{for any } r > 0, \quad (2.28)$$

with f given in (2.26). Similarly we find

$$G(s, r) = \int_s^{h(s,r)} -\frac{\beta}{2g(h)} dh = \begin{cases} -\frac{1}{2\delta_1} \ln \frac{h(s,r)(\delta_1 + \delta_2 \beta s)}{s(\delta_1 + \delta_2 \beta h(s,r))}, & s > 0, \\ 0, & s = 0. \end{cases} \quad (2.29)$$

Substituting (2.27) and (2.29) into (2.13) we get the following second-order time-splitting sine-spectral steps for the NLS with a combination of cubic and quintic damping terms

$$\begin{aligned} \psi_j^* &= \begin{cases} \frac{\sqrt{h(|\psi_j^n|^2, k/2)}}{|\psi_j^n|} \exp \left\{ i \left[-\frac{V(x_j)k}{2} - \frac{1}{2\delta_1} \ln \frac{h(|\psi_j^n|^2, k/2)(\delta_1 + \delta_2 \beta |\psi_j^n|^2)}{|\psi_j^n|^2(\delta_1 + \delta_2 \beta h(|\psi_j^n|^2, k/2))} \right] \right\} \psi_j^n, & \psi_j^n \neq 0, \\ 0, & \psi_j^n = 0, \end{cases} \\ \psi_j^{**} &= \sum_{l=1}^{M-1} e^{-ik\mu_l^2/2} \widehat{\psi}_l^* \sin(\mu_l(x_j - a)), \quad j = 1, 2, \dots, M-1, \\ \psi_j^{n+1} &= \begin{cases} \frac{\sqrt{h(|\psi_j^{**}|^2, k/2)}}{|\psi_j^{**}|} \exp \left\{ i \left[-\frac{V(x_j)k}{2} - \frac{1}{2\delta_1} \ln \frac{h(|\psi_j^{**}|^2, k/2)(\delta_1 + \delta_2 \beta |\psi_j^{**}|^2)}{|\psi_j^{**}|^2(\delta_1 + \delta_2 \beta h(|\psi_j^{**}|^2, k/2))} \right] \right\} \psi_j^{**}, & \psi_j^{**} \neq 0, \\ 0, & \psi_j^{**} = 0. \end{cases} \end{aligned} \quad (2.30)$$

Remark 2.1 *As demonstrated in this subsection, the integrals in (2.7) and (2.12) can be evaluated **analytically** for the damping terms which most frequently appear in physical applications. If the integrals in (2.7) or (2.12) can not be evaluated analytically or the inverse of f in (2.7) can not be expressed explicitly, e.g., if $g(\rho)$ in (1.5) is not a polynomial, one can solve the following ODE numerically by either second- or fourth-order Runge-Kutta method*

$$\begin{aligned} \frac{dh(t)}{dt} &= -2g(h(t)) h(t), & 0 \leq t \leq k/2, \\ h(0) &= s, \end{aligned}$$

to get $h(s, k/2)$ for any given $s > 0$ and set $h(s, k/2) = 0$ for $s = 0$. By changing the variable of integration in (2.12), see detail in (2.27) and (2.29), the first integral in (2.12), i.e. $F(s, k/2)$, can be evaluated exactly (see detail in (2.27)), and the second integral in (2.12), i.e. $G(s, k/2) = \int_s^{h(s, k/2)} -\frac{\beta h^{\sigma-1}}{2g(h)} dh$, can be evaluated numerically by using a numerical quadrature, e.g., the trapezoidal rule or Simpson's rule.

The scheme TSSP is explicit and is unconditionally stable as we will demonstrate in the next subsection. Another main advantage of the time-splitting method is its time transversal invariance, which also holds for the NLS and the damped NLS themselves. If a constant α is added to the potential V , then the discrete wave functions $\psi_j^{\varepsilon, n+1}$ obtained from TSSP get multiplied by the phase factor $e^{-i\alpha(n+1)k}$, which leaves the discrete normalization unchanged. This property does not hold for finite difference schemes.

Remark 2.2 *For the focusing cubic NLS with a quintic damping term describing three-body recombination loss and an additional feeding term for the BEC [27] we choose $\sigma = 1$, $g(\rho) = -\delta_1 + \delta_2\beta^2\rho^2$ with $\delta_1, \delta_2 > 0$ in (1.5). The idea of constructing the TSSP is also applicable to this case although we could not prove that it is unconditionally stable due to the feeding term. Inserting the above feeding term into (2.7), we get*

$$f(s) = \begin{cases} \frac{1}{2\delta_1} \ln |\delta_2\beta^2 - \delta_1/s^2|, & s > 0, \\ 0, & s = 0. \end{cases} \quad (2.31)$$

Inserting (2.31) into (2.9), we find

$$h(s, \tau) = \frac{s\sqrt{\delta_1}}{\sqrt{\delta_1 e^{-4\tau\delta_1} + (1 - e^{-4\tau\delta_1})\delta_2\beta^2 s^2}}, \quad (2.32)$$

and substituting (2.32) into (2.9) and (2.12), we obtain

$$\rho(t) = \frac{|\psi(x, t_n)|^2 \sqrt{\delta_1}}{\sqrt{\delta_1 e^{-4\tau\delta_1} + (1 - e^{-4\tau\delta_1})\delta_2\beta^2 |\psi(x, t_n)|^4}}, \quad t_n \leq t \leq t_{n+1}, \quad (2.33)$$

$$F(s, r) = -\delta_1 r + \frac{1}{4} \ln \left[1 + \delta_2 \beta^2 s^2 (e^{4\delta_1 r} - 1) / \delta_1 \right], \quad (2.34)$$

$$G(s, r) = \frac{1}{2\sqrt{\delta_1 \delta_2}} \ln \frac{\beta s \sqrt{\delta_2} e^{2r\delta_1} + \sqrt{\delta_1 + \delta_2 \beta^2 s^2 (e^{4r\delta_1} - 1)}}{\sqrt{\delta_1} + \beta s \sqrt{\delta_2}}. \quad (2.35)$$

Inserting (2.34) and (2.35) into (2.13), we get the following second-order time-splitting sine-spectral steps for the NLS with a quintic damping term and a feeding term

$$\begin{aligned} \psi_j^* &= \frac{e^{k\delta_1/2} \exp \left[i \left(-\frac{V(x_j)k}{2} + \frac{1}{2\sqrt{\delta_1 \delta_2}} \ln \frac{\beta |\psi_j^n|^2 \sqrt{\delta_2} e^{k\delta_1} + \sqrt{\delta_1 + \delta_2 \beta^2 |\psi_j^n|^4 (e^{2k\delta_1} - 1)}}{\sqrt{\delta_1} + \beta |\psi_j^n|^2 \sqrt{\delta_2}} \right) \right]}{\left[1 + \delta_2 \beta^2 |\psi_j^n|^4 (e^{2k\delta_1} - 1) / \delta_1 \right]^{1/4}} \psi_j^n, \\ \psi_j^{**} &= \sum_{l=1}^{M-1} e^{-ik\mu_l^2/2} \widehat{\psi}_l^* \sin(\mu_l(x_j - a)), \quad j = 1, 2, \dots, M-1, \\ \psi_j^{n+1} &= \frac{e^{k\delta_1/2} \exp \left[i \left(-\frac{V(x_j)k}{2} + \frac{1}{2\sqrt{\delta_1 \delta_2}} \ln \frac{\beta |\psi_j^{**}|^2 \sqrt{\delta_2} e^{k\delta_1} + \sqrt{\delta_1 + \delta_2 \beta^2 |\psi_j^{**}|^4 (e^{2k\delta_1} - 1)}}{\sqrt{\delta_1} + \beta |\psi_j^{**}|^2 \sqrt{\delta_2}} \right) \right]}{\left[1 + \delta_2 \beta^2 |\psi_j^{**}|^4 (e^{2k\delta_1} - 1) / \delta_1 \right]^{1/4}} \psi_j^{**}. \end{aligned} \quad (2.36)$$

Remark 2.3 The scheme TSSP (2.13) can easily be extended for solving the complex Ginzburg-Landau equation (CGL) [17, 30]

$$i \psi_t = -(1 - i \varepsilon) \Delta \psi - |\psi|^2 \psi - i (\delta_2 |\psi|^2 - \delta_1) \psi, \quad (2.37)$$

where ε , δ_1 and δ_2 are positive constants. The idea of constructing the TSSP for the damped NLS is also applicable to the CGL provided that we solve

$$i \psi_t = -(1 - i \varepsilon) \Delta \psi, \quad (2.38)$$

in the first step instead of (2.3). Inserting $\sigma = 1$, $\beta = 1$ and $g(\rho) = \delta_2 \rho - \delta_1$ with $\delta_1, \delta_2 > 0$ into (1.5) and using (2.7) we get

$$f(s) = \begin{cases} \frac{1}{\delta_1} \ln |\delta_2 - \delta_1/s|, & s > 0, \\ 0, & s = 0. \end{cases} \quad (2.39)$$

Inserting (2.39) into (2.7) we find

$$h(s, \tau) = \frac{s\delta_1}{s\delta_2 (1 - e^{-2\tau\delta_1}) + \delta_1 e^{-2\tau\delta_1}}, \quad (2.40)$$

and substituting (2.40) into (2.9) and (2.12) we obtain

$$\rho(t) = \frac{\delta_1 |\psi(x, t_n)|^2}{\delta_2 |\psi(x, t_n)|^2 (1 - e^{-2\tau\delta_1}) + \delta_1 e^{-2\tau\delta_1}}, \quad t_n \leq t \leq t_{n+1}, \quad (2.41)$$

$$F(s, r) = -\frac{1}{2} \ln \frac{\delta_1}{s\delta_2 + (\delta_1 - s\delta_2) e^{-2r\delta_1}}, \quad (2.42)$$

$$G(s, r) = \frac{1}{2\delta_2} \ln \frac{\delta_1 - s\delta_2 + s\delta_2 e^{2r\delta_1}}{\delta_1}. \quad (2.43)$$

Inserting (2.42) and (2.43) into (2.13), we get the following second-order time-splitting sine-spectral steps for the CGL (2.37)

$$\begin{aligned}
\psi_j^* &= \sqrt{\frac{\delta_1}{\delta_2|\psi_j^n|^2 + (\delta_1 - \delta_2|\psi_j^n|^2)e^{-k\delta_1}}} \exp\left[\frac{i}{2\delta_2} \ln \frac{\delta_1 - \delta_2|\psi_j^n|^2 + \delta_2|\psi_j^n|^2 e^{k\delta_1}}{\delta_1}\right] \psi_j^n, \\
\psi_j^{**} &= \sum_{l=1}^{M-1} e^{-(\varepsilon+i)k\mu_l^2} \widehat{\psi}_l^* \sin(\mu_l(x_j - a)), \quad j = 1, 2, \dots, M-1, \\
\psi_j^{n+1} &= \sqrt{\frac{\delta_1}{\delta_2|\psi_j^{**}|^2 + (\delta_1 - \delta_2|\psi_j^{**}|^2)e^{-k\delta_1}}} \exp\left[\frac{i}{2\delta_2} \ln \frac{\delta_1 - \delta_2|\psi_j^{**}|^2 + \delta_2|\psi_j^{**}|^2 e^{k\delta_1}}{\delta_1}\right] \psi_j^{**},
\end{aligned} \tag{2.44}$$

Remark 2.4 If the homogeneous periodic boundary conditions in (2.2) are replaced by the periodic boundary conditions

$$\psi(a, t) = \psi(b, t), \quad \psi_x(a, t) = \psi_x(b, t), \quad t \geq 0, \tag{2.45}$$

the TSSP scheme (2.13) still works provided that one replaces the sine-series in (2.13) by a Fourier-series [7, 6, 8].

2.3 Stability and decay rate

Let $U = (U_0, U_1, \dots, U_M)^T$ with $U_0 = U_M = \mathbf{0}$ and $\|\cdot\|_{l^2}$ be the usual discrete l^2 -norm on the interval (a, b) , i.e.,

$$\|U\|_{l^2} = \sqrt{\frac{b-a}{M} \sum_{j=1}^{M-1} |U_j|^2}. \tag{2.46}$$

For the *stability* of the time-splitting sine-spectral approximations TSSP (2.13), we have the following lemma, which shows that the total normalization does not increase.

Lemma 2.1 *The time-splitting sine-spectral schemes (TSSP) (2.13) are unconditionally stable if $g(s) \geq 0$ for $s \geq 0$. In fact, for every mesh size $h > 0$ and time step $k > 0$,*

$$\|\psi^{n+1}\|_{l^2} \leq \|\psi^n\|_{l^2} \leq \|\psi^0\|_{l^2} = \|\psi_0\|_{l^2}, \quad n = 0, 1, 2, \dots \tag{2.47}$$

Furthermore, when a linear damping term is used in (1.5), i.e., we choose $g(\rho) \equiv \delta$ with $\delta > 0$, the decay rate of the normalization satisfies

$$\|\psi^n\|_{l^2} = e^{-2\delta t_n} \|\psi^0\|_{l^2} = e^{-2\delta t_n} \|\psi_0\|_{l^2}, \quad n = 1, 2, \dots \tag{2.48}$$

In fact, (2.48) is a discretized version of the decay rate of the normalization $N(t)$ in (1.8).

Proof: We combine (2.13), (2.14), (2.46) and note that $F(s, \tau) \geq 0$ for $s \geq 0$ and $\tau \geq 0$, to obtain

$$\begin{aligned}
\frac{1}{b-a} \|\psi^{n+1}\|_{l^2}^2 &= \frac{1}{M} \sum_{j=1}^{M-1} |\psi_j^{n+1}|^2 \\
&= \frac{1}{M} \sum_{j=1}^{M-1} \exp[-2F(|\psi_j^{**}|^2, k/2)] |\psi_j^{**}|^2 \leq \frac{1}{M} \sum_{j=1}^{M-1} |\psi_j^{**}|^2 \\
&= \frac{1}{M} \sum_{j=1}^{M-1} \left| \sum_{l=1}^{M-1} e^{-ik\mu_l^2/2} \hat{\psi}_l^* \sin(\mu_l(x_j - a)) \right|^2 = \frac{1}{2} \sum_{l=1}^{M-1} |e^{-ik\mu_l^2/2} \hat{\psi}_l^*|^2 = \frac{1}{2} \sum_{l=1}^{M-1} |\hat{\psi}_l^*|^2 \\
&= \frac{1}{2} \sum_{l=1}^{M-1} \left| \frac{2}{M} \sum_{j=1}^{M-1} \psi_j^* \sin(\mu_l(x_j - a)) \right|^2 = \frac{1}{M} \sum_{j=1}^{M-1} |\psi_j^*|^2 \\
&= \frac{1}{M} \sum_{j=1}^{M-1} \exp[-2F(|\psi_j^n|^2, k/2)] |\psi_j^n|^2 \leq \frac{1}{M} \sum_{j=1}^{M-1} |\psi_j^n|^2 \\
&= \frac{1}{b-a} \|\psi^n\|_{l^2}^2. \tag{2.49}
\end{aligned}$$

Here, we used the identity

$$\sum_{j=1}^{M-1} \sin\left(\frac{\pi r j}{M}\right) \sin\left(\frac{\pi s j}{M}\right) = \begin{cases} 0, & r - s \neq 2mM, \\ M/2, & r - s = 2mM, r \neq 2nM, \end{cases} \quad m, n \text{ integer.} \tag{2.50}$$

When a linear damping term is added to the NLS (1.5), the equality (2.48) follows from the above proof, Eq. (2.18), and

$$\sum_{j=1}^{M-1} \exp[-2F(|\psi_j^n|^2, k/2)] |\psi_j^n|^2 = \sum_{j=1}^{M-1} e^{-\delta k} |\psi_j^n|^2 = e^{-\delta k} \sum_{j=1}^{M-1} |\psi_j^n|^2.$$

3 Numerical examples

In this section we present numerical tests of the TSSP (2.13) for solving a focusing cubic NLS appearing in nonlinear optics [18, 38] and for the Gross-Pitaeskkii equation in BEC [8] in 2d with a linear, a cubic, or a quintic damping term. In our computations, the initial condition (1.2) is always chosen such that $|\psi_0(\mathbf{x})|$ decays to zero sufficiently fast as $|\mathbf{x}| \rightarrow \infty$. We choose an appropriately large rectangle $[a, b] \times [c, d]$ in 2d to avoid that the homogeneous periodic boundary condition (2.2) introduce a significant (aliasing) error relative to the whole space problem. To quantify the numerical results of the GPE for a BEC, we define the condensate widths along the x , y and z -axis by

$$\sigma_\alpha^2 = \langle \alpha^2 \rangle = \frac{1}{N(t)} \int_{\mathbb{R}^d} \alpha^2 |\psi(\mathbf{x}, t)|^2 d\mathbf{x}, \quad \text{with } \alpha = x, y, \text{ or } z.$$

Example 1 Solution of the 2d damped focusing cubic nonlinear Schrödinger equation. We choose $d = 2$, $\sigma = 1$ and $V(x, y) \equiv 0$ in (1.5) and present computations for three different damping terms ($\delta > 0$):

- I. A linear damping term, i.e. we choose $g(\rho) \equiv \delta$.
- II. A cubic damping term, i.e. we choose $g(\rho) \equiv \delta\beta\rho$.
- III. A quintic damping term, i.e. we choose $g(\rho) \equiv \delta\beta^2\rho^2$.

The initial condition (1.6) is taken to be

$$\psi(x, y, 0) = \psi_0(x, y) = \frac{\gamma_y^{1/4}}{\sqrt{\pi\varepsilon}} e^{-(x^2 + \gamma_y y^2)/2\varepsilon}, \quad (x, y) \in \mathbb{R}^2. \quad (3.1)$$

We assume $\gamma_y = 2$, $\varepsilon = 0.2$ and $\beta = 8$ in (1.5) such that $E(0) = -0.751582 < 0$ in (1.4). We solve the NLS on the square $[-16, 16]^2$, i.e., $a = c = -16$ and $b = d = 16$ with mesh size $h = \frac{1}{32}$, time step $k = 0.0002$ and homogeneous periodic boundary conditions along the boundary of the square. We compare the effect of changing the damping parameter δ in the three different cases I, II and III.

Figure 1 shows the surface plot of the density $|\psi(x, y, t)|^2$ at time $t = 1.25$ with $\delta = 0.5$; plots of the normalization, energy and central density $|\psi(0, 0, t)|^2$ as functions of time with $\delta = 0.5$, 0.3 and $\delta = 0$ (no damping) for case I. Figure 2 shows similar results for case II and Figure 3 for case III. Furthermore Figure 4 shows contour plots of the density $|\psi|^2$ at different times for case III with $\delta = 0.01$.

In the numerically computations, a blowup is detected either from the plot of the central density $|\psi(0, 0, t)|^2$ which at the blowup shows a very sharp spike with a peak value that increases when the mesh size h decreases, or from the plot of the energy $E(t)$ which has a very sharp spike with negative values at the blowup. In fact, the method TSSP (2.13) aims to capture the solution of damped NLS without blowup, i.e. physical relevant solution. If one wants to capture the blowup rate of NLS, we refer to [29, 33].

From the numerical results we find the following conditions for arresting a blowup of the wave function with initial energy $E(0) < 0$. (1) For linear damping the blowup is arrested if the damping parameter is bigger than a certain threshold value which we find to be $\delta_{\text{th}} \approx 0.461$ by numerical experiments. As shown in Fig. 1b blowup is arrested for $\delta = 0.5 > \delta_{\text{th}}$ while the wave function blows up for $\delta < \delta_{\text{th}}$ as can be seen from Fig. 1c&d where we have chosen $\delta = 0.3 < \delta_{\text{th}}$ and $\delta = 0 < \delta_{\text{th}}$, respectively. The time at which the blowup of the wave function happens, however, increases with increasing δ (cf. Fig. 1c&d). (2) For a cubic damping term with $\delta > 0$ the blowup of the wave function is always arrested (cf. Fig. 2). (3) The above observation (2) also holds for a quintic damping term (cf. Fig. 3).

For linear damping, we also test the dependence of the threshold value of the damping parameter δ_{th} on β and the initial data. First we take $\gamma_y = 2$ and $\varepsilon = 0.2$ in (3.1). Table 1 shows the threshold values δ_{th} for different β in (1.5), and $E(0)$

	$\beta = 8$	$\beta = 16$	$\beta = 32$	$\beta = 64$	$\beta = 128$
$E(0)$	-0.7516	-5.253	-14.256	-32.263	-68.275
δ_{th}	0.461	3.655	10.35	22.15	40.05

Table 1: Dependence of δ_{th} on β for $\gamma_y = 2$ and $\varepsilon = 0.2$ in (3.1).

	$\varepsilon = 0.8$	$\varepsilon = 0.4$	$\varepsilon = 0.2$	$\varepsilon = 0.1$	$\varepsilon = 0.05$
$E(0)$	-1.3133	-2.6266	-5.2532	-10.506	-21.013
δ_{th}	0.895	1.845	3.655	7.25	14.55

Table 2: Dependence of δ_{th} on ε in (3.1) for $\beta = 16$ in (1.5) and $\gamma_y = 2$ in (3.1).

represents the initial energy. Then we choose $\beta = 16$ in (1.5) and $\gamma_y = 2$ in (3.1). Table 2 displays the threshold values δ_{th} for different values of ε in (3.1).

From Table 1 we find by a least square fitting,

$$\delta_{\text{th}} = -0.6930E(0) \quad \text{or} \quad \delta_{\text{th}} = 0.3872\beta - 2.4627.$$

Similarly, from Table 2 we obtain

$$\delta_{\text{th}} = -0.6922E(0).$$

Based on this observation, we conclude that the threshold value of the linear damping parameter δ_{th} depends linearly on the initial energy $E(0)$.

Example 2 Solution of the 2d damped GPE with focusing nonlinearity. We choose $d = 2$, $\sigma = 1$ and $V(x, y) = \frac{1}{2}(\gamma_x^2 x^2 + \gamma_y^2 y^2)$ to be a harmonic oscillator potential with $\gamma_x, \gamma_y > 0$ in (1.5). Again, we present computations for the same three different damping terms in (1.5) as those we studied in Example 1.

We take $\gamma_x = 1$ and $\gamma_y = 4$. The initial condition (1.6) is assumed to be the ground-state solution of (1.5) with $g(\rho) \equiv 0$ (i.e. undamped case) and $\beta = -40$. The cubic nonlinearity is ramped linearly from $\beta = -40$ (defocusing) to $\beta = 50$ (focusing) during the time interval $[0, 0.1]$ and afterwards kept constant. The absorption parameter was set to $\delta = 0$ during the time interval $[0, 0.1]$ and increased to a positive value $\delta > 0$ afterwards.

We solve the GPE on the rectangle $[-24, 24] \times [-6, 6]$, i.e., for $a = -24$, $b = 24$, $c = -6$ and $d = 6$ with mesh size $h_x = \frac{3}{64}$, $h_y = \frac{3}{128}$, time step $k = 0.0005$ and homogeneous periodic boundary conditions along the boundary of the rectangle. Again, we compare the effect of changing the damping parameter δ in the three different cases I, II and III.

Figure 5 shows a surface plot of the density $|\psi(x, y, t)|^2$ at times $t = 0$ (ground-state solution) and $t = 2.8$ with $\delta = 1.25$; normalization, energy and central density $|\psi(0, 0, t)|^2$ as functions of time with $\delta = 1.25, 1.1$ and 0 (no damping) for case I.

Figure 6 shows similar results for case II and Figure 7 for case III. Furthermore Figure 8 shows contour plots of the density $|\psi|^2$ at different times for case III with $\delta = 0.15$.

From our numerical results we find that the observations (1)-(3) made for example 1 are still valid with the additional trapping potential. However, the value of δ_{th} , depends on β (or initial energy $E(0)$) and we find $\delta_{\text{th}} \approx 1.185$ for linear damping (cf. Fig. 5).

3.1 Discussion

In this subsection we discuss our numerical results in terms of physical properties of a BEC described by the GPE. We concentrate on those cases where a collapse of the wave function is arrested since this collapse leads to unphysical processes like the negative peaks in the energy $E(t)$ shown in Figs. 1c&d,5e&f.

The general form of the time evolution in example 1 is similar for all three cases. Initially the cloud of atoms contracts due to the attractive interaction between the particles. This contraction is accompanied by an increase in the energy due to particle loss which is most efficient in regions of high particle density. These regions are characterized by a negative local energy density leading to an increase in energy for each particle lost there. After the central particle density has reached a maximum the cloud starts to expand due to the kinetic energy gained by the particles during the contraction. Particles are emitted from the cloud in burst like pulses which can be seen in Figs. 4,8. Such bursts have also been seen in BEC experiments [13]. The main differences between the three cases are the behavior of the energy and the number of particles as a function of time. In case I where we assumed a linear damping term the loss rate of particles from the condensate is independent of the shape of the condensate wave function. The energy decrease during the condensate expansion is determined by the loss of particles (cf. Fig. 1b). In the cases of cubic and quintic damping the loss term only has a significant effect on the time evolution of the condensate during the contraction. When the condensate expands the density of particles is so low that the loss terms have only a very small effect and the energy $E(t)$ and the number of particles $N(t)$ remain almost constant (see Figs. 2c,3c&d).

In example 2 we add an additional trap potential which confines the BEC and assume a realistic scenario (described above) to prepare the condensate in the trap (cf. experiments by Donley *et al.* [13]). We find that the initial process of turning on the attractive interactions between the particles leads to oscillations in the widths of the condensate [8] as can be seen from Figs. 5,6,7. However, neither the additional trap potential nor these oscillations significantly alter the behavior of the system compared to example 1 when the condensate is strongly contracted. Before and after this contraction some differences can be seen. By looking at Figs. 5,6 we find that the first minimum in σ_y due to the oscillations of the condensate causes an increase in the central density and in the energy. For cubic and quintic damping this is accompanied by an increased particle loss. However, an arrested collapse of the

wave function only happens when both σ_x and σ_y attain a minimum value due to the attractive interactions (cf. Fig. 5d and Fig. 6b). We also note that the frequency of the oscillations after an arrested collapse has happened is not significantly influenced by the damping terms. The amplitude of these oscillations is, however, strongly dependent on δ and decreases with increasing δ . Finally, we want to mention that a series of contractions and expansion of the condensate is possible. In Fig. 7b we find three contractions of the condensate where only the first one reaches a sufficiently high particle density to lead to an increase in energy while the next two contractions show a rather smooth decrease in energy and particle number. For a smaller quintic damping term we obtain two contractions of the condensate which increase the energy (see Fig. 7c).

4 Conclusions

We extended the explicit unconditionally stable second-order time-splitting sine-spectral (TSSP) method for solving damped focusing nonlinear Schrödinger equations. We showed that this method is time transversal invariant and preserves the exact decay rate of the normalization for a linear damping of the NLS. Extensive numerical tests were presented for the cubic focusing nonlinear Schrödinger equation in 2d with linear, cubic and quintic damping terms. Our numerical results show that quintic damping always arrests blowup, whereas linear and cubic damping can arrest blowup only when the damping parameter δ is bigger than a certain threshold value δ_{th} . We will apply this novel method to solve the 3d Gross-Pitaevskii equation with a quintic damping term and compare the numerical results with the experimental dynamics [13] of collapsing and exploding BECs [9].

Acknowledgment

W.B. acknowledges support by the National University of Singapore grant No. R-151-000-027-112. This work was supported by the WITTGENSTEIN-AWARD of P. Markowich and P. Zoller which is funded by the Austrian National Science Foundation FWF. The authors also acknowledge hospitality of the International Erwin Schrödinger Institute in Vienna where this work was initiated.

References

- [1] S.K. Adhikari, Mean-field theory for collapsing and exploding Bose-Einstein condensates, preprint.
- [2] G.D. Akrivis, V.A. Dougalis, O.A. Karakashian and W.R. Mckinney, Numerical approximation of singular solutions of the damped nonlinear Schrödinger equation, ENUMATH'97 (Heidelberg), World Scientific, River Edge, NJ, 1998, pp. 117-124.

- [3] M.H. Anderson, J.R. Ensher, M.R. Matthews, C.E. Wieman, and E.A. Cornell, Observation of Bose-Einstein condensation in a dilute atomic vapor, *Science*, 269(1995), pp. 198-201.
- [4] J.R. Anglin and W. Ketterle, Bose-Einstein condensation of atomic gases, *Nature*, 416(2002), pp. 211-218.
- [5] W. Bao, S. Jin and P.A. Markowich, On time-splitting spectral approximations for the Schrödinger equation in the semiclassical regime, *J. Comput. Phys.*, 175(2002), pp. 487-524.
- [6] W. Bao, S. Jin and P.A. Markowich, Numerical study of time-splitting spectral discretizations of nonlinear Schrödinger equations in the semi-classical regimes, *SIAM J. Sci. Comp.*, to appear.
- [7] W. Bao and W. Tang, Ground state solution of trapped interacting Bose-Einstein condensate by minimizing a functional, *J. Comput. Phys.*, in press.
- [8] W. Bao, D. Jaksch and P.A. Markowich, Numerical solution of the Gross-Pitaevskii equation for Bose-Einstein condensation, *J. Comput. Phys.*, in press.
- [9] W. Bao *et al.*, in preparation.
- [10] R. Ciegis and V. Pakalnyte, The finite difference scheme for the solution of weakly damped nonlinear Schrödinger equation, *Internat. J. Appl. Sci. Comput.*, 8(2001), pp. 127-134.
- [11] E. Cornell, Very cold indeed: The nanokelvin physics of Bose-Einstein condensation, *J. Res. Natl. Inst. Stan.*, 101(1996), pp. 419-434.
- [12] F. Dalfovo, S. Giorgini, L.P. Pitaevskii and S. Stringari, *Rev. Mod. Phys.* 71(1999), 463.
- [13] E.A. Donley, N.R. Claussen, S.L. Cornish, J.L. Roberts, E.A. Cornell and C.E. Wieman, Dynamics of collapsing and exploding Bose-Einstein condensates, *Nature*, 412(2001), pp. 295-299.
- [14] R.A. Duine, H.T.C. Stoof, Explosion of a collapsing Bose-Einstein condensate, *Phys. Rev. Lett.*, 86(2001), pp. 2204-2207.
- [15] M. Edwards and K. Burnett, Numerical solution of the nonlinear Schrödinger equation for small samples of trapped neutral atoms, *Phys. Rev. A*, 51(1995), pp. 1382-1386.
- [16] G. Fibich, Self-focusing in the damped nonlinear Schrödinger equation, *SIAM J. Appl. Math.*, 61(2001), pp. 1680-1705.

- [17] G. Fibich and D. Levy, Self-focusing in the complex Ginzburg-Landau limit of the critical nonlinear Schrödinger equation, *Phys. Lett. A*, 249(1998), pp. 286-294.
- [18] G. Fibich and G. Papanicolaou, Self-focusing in the perturbed and unperturbed nonlinear Schrödinger equation in critical dimension, *SIAM J. Appl. Math.*, 60(2000), pp. 183-240.
- [19] O. Goubet, Asymptotic smoothing effect for a weakly damped nonlinear Schrödinger equation in T^2 , *J. Diff. Equ.*, 165(2000), pp. 96–122.
- [20] O. Goubet, Regularity of the attractor for a weakly damped nonlinear Schrödinger equation in R^2 , *Adv. Diff. Equ.*, 3(1998), pp. 337–360.
- [21] O. Goubet, Approximate inertial manifolds for a weakly damped nonlinear Schrödinger equation, *Discrete Contin. Dynam. Systems*, 3(1997), pp. 503–530.
- [22] M. Greiner, O. Mandel, T. Esslinger, T.W. Hänsch, and I. Bloch, Quantum phase transition from a superfluid to a mott insulator in a gas of ultracold atoms, *Nature*, 415(2002), pp. 39-45.
- [23] E.P. Gross, *Nuovo. Cimento.*, 20(1961), 454.
- [24] S.R.K. Iyengar, G. Jayaraman and V. Balasubramanian, Variable mesh difference schemes for solving a nonlinear Schrödinger equation with a linear damping term. *Advances in partial differential equations, III. Comput. Math. Appl.*, 40(2000), pp. 1375-1385.
- [25] D. Jaksch, C. Bruder, J. I. Cirac, C. W. Gardiner, and P. Zoller, Cold bosonic atoms in optical lattices, *Phys. Rev. Lett.*, 81(1998), pp. 3108-3111.
- [26] M.S. Jolly, R. Temam and C. Xiong, An application of approximate inertial manifolds to a weakly damped nonlinear Schrödinger equation, *Numer. Funct. Anal. Optim.*, 16(1995), pp. 923-937.
- [27] Y. Kagan, A.E. Muryshev and G.V. Shlyapnikov, *Phys. Rev. Lett.*, Collapse and Bose-Einstein condensation in a trapped Bose gas with negative scattering length, 81(1998), pp. 933-937.
- [28] L. Landau and E. Lifschitz, *Quantum Mechanics: non-relativistic theory*, Pergamon Press, New York, 1977.
- [29] M.J. Landman, G.C. Papanicolaou, C. Sulem, P.L. Sulem, X.P. Wang, Stability of isotropic singularities for the nonlinear Schrödinger equation, *Phys. D*, 47 (1991), pp. 393–415.

- [30] A. Mielke, The complex Ginzburg-Landau equation on large and unbounded domains: sharper bounds and attractors, *Nonlinearity*, 10(1997), pp. 199-222.
- [31] G. Moebis, Guy A multilevel method for the resolution of a stochastic weakly damped nonlinear Schrödinger equation, *Appl. Numer. Math.*, 26(1998), pp. 353-375.
- [32] G. Moebis and R. Temam, Resolution of a stochastic weakly damped nonlinear Schrödinger equation by a multilevel numerical method, *J. Opt. Soc. Amer. A*, 17(2000), pp. 1870-1879.
- [33] G.C. Papanicolaou, C. Sulem, P.L. Sulem, X.P. Wang, Singular solutions of the Zakharov equations for Langmuir turbulence, *Phys. Fluids B*, 3 (1991), pp. 969-980.
- [34] L.S. Peranich, A finite difference scheme for solving a non-linear Schrödinger equation with a linear damping term, *J. Comput. Phys.*, 68(1987), pp. 501-505.
- [35] L.P. Pitaevskii, *Zh. Eksp. Teor. Fiz.*, 40(1961), 646. (*Sov. Phys. JETP*, 13(1961), 451).
- [36] J.L. Roberts, N.R. Claussen, S.L. Cornish and C.E. Wieman, Magnetic field dependence of ultracold inelastic collisions near a Feshbach resonance, preprint.
- [37] H. Saito and M. Ueda, Intermittent implosion and pattern formation of trapped Bose-Einstein condensates with an attractive interaction, *Phys. Rev. Lett.*, 86(2001), pp. 1406-1409.
- [38] C. Sulem and P.L. Sulem, *The Nonlinear Schrödinger Equation: Self-focusing and Wave Collapse*, Springer, New York, 1999.
- [39] M. Tsutsumi, Nonexistence of global solutions to the Cauchy problem for the damped nonlinear Schrödinger equations, *SIAM J. Math. Anal.*, 15(1984), pp. 357-366.
- [40] M. Tsutsumi, On global solutions to the initial-boundary value problem for the damped nonlinear Schrödinger equations, *J. Math. Anal. Appl.*, 145(1990), pp. 328-341.
- [41] F.Y. Zhang and S.J. Lu, Long-time behavior of finite difference solutions of a nonlinear Schrödinger equation with weakly damped, *J. Comput. Math.*, 19(2001), pp. 393-406.

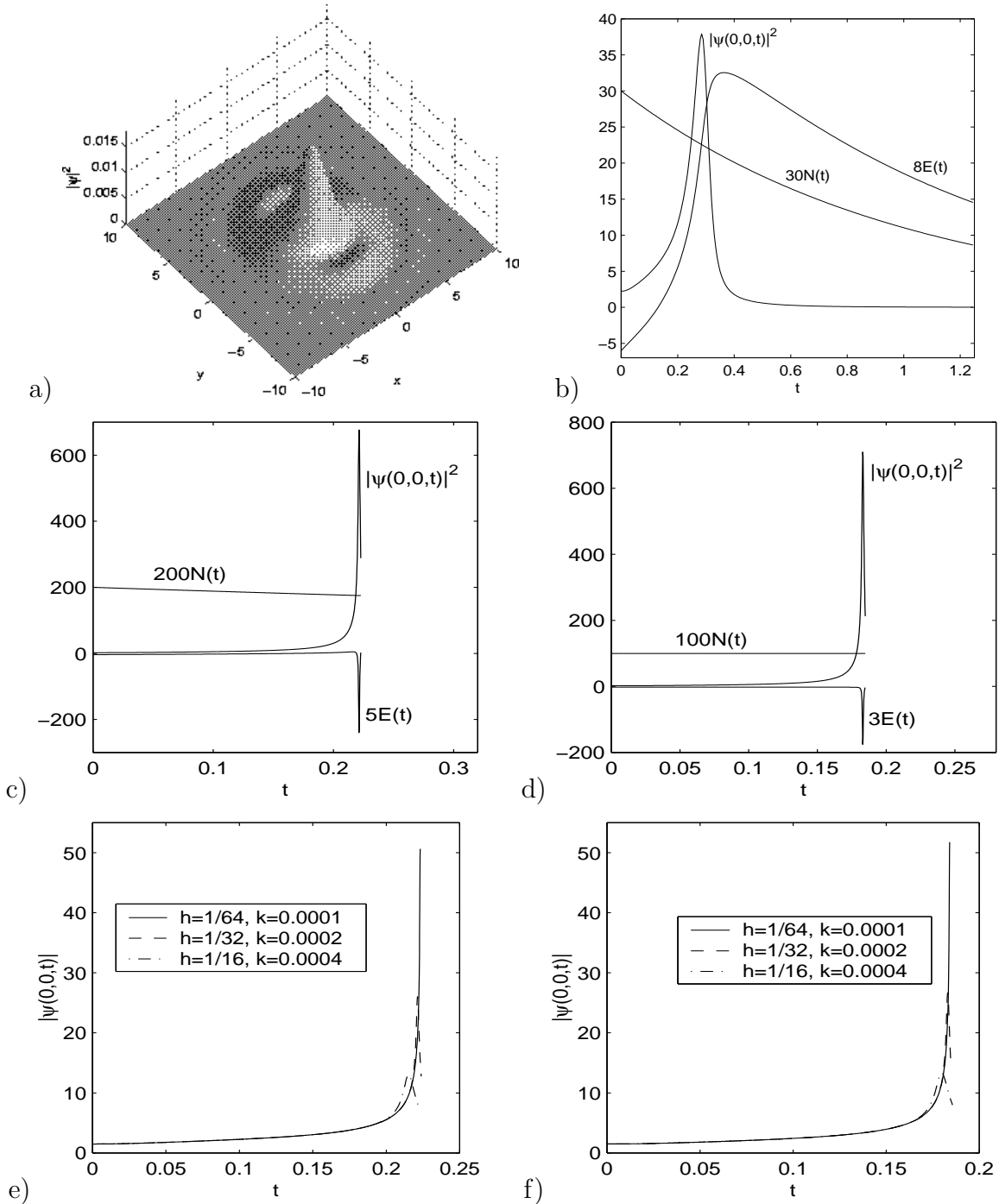


Figure 1: Numerical results in Example 1 case I. a). Surface plot of the density $|\psi|^2$ at time $t = 1.25$ with $\delta = 0.5$. Normalization, energy and central density $|\psi(0,0,t)|^2$ as functions of time: b). with $\delta = 0.5$, c). $\delta = 0.3$, d). $\delta = 0$ (no damping). Blowup study: e). $\delta = 0.3$, f). $\delta = 0$ (no damping).

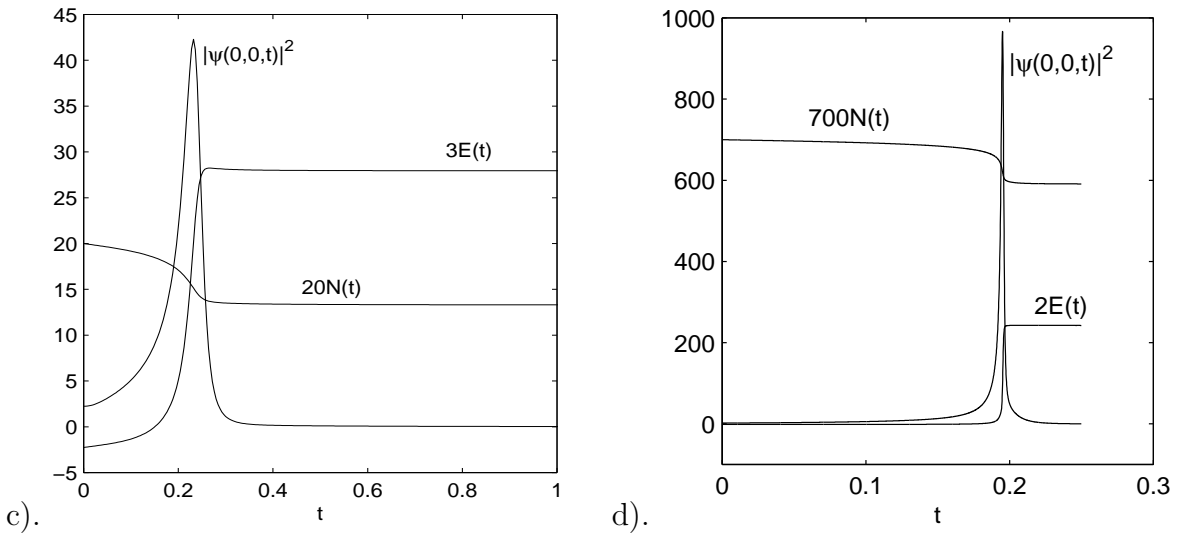
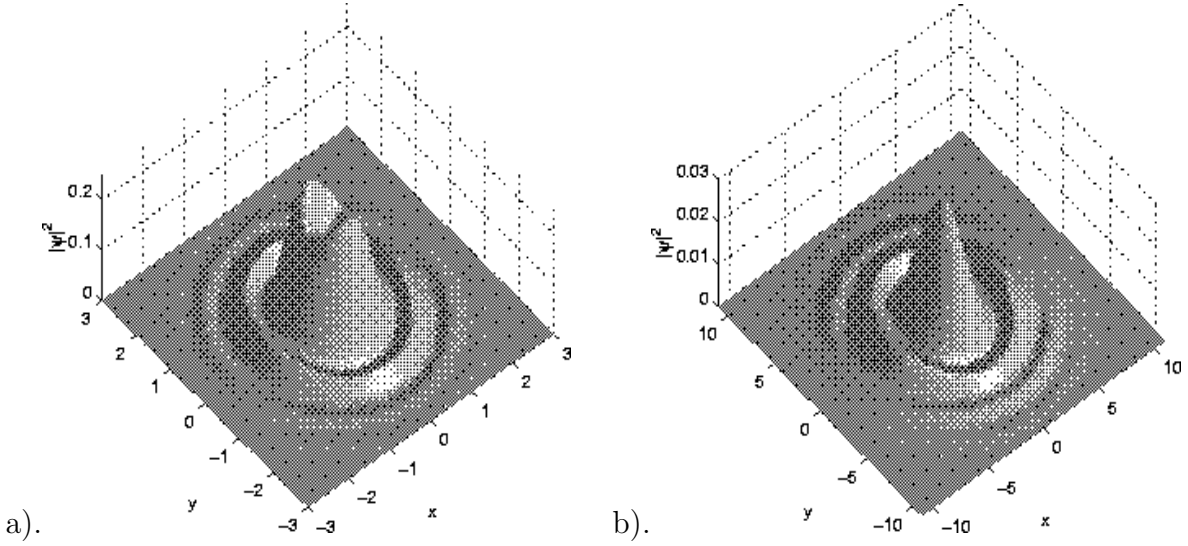


Figure 2: Numerical results in Example 1 case II. Surface plot of the density $|\psi|^2$ with $\delta = 0.02$: a). At time $t = 0.4$, b). $t = 1.0$. Normalization, energy and central density $|\psi(0,0,t)|^2$ as functions of time: c). with $\delta = 0.02$, d). $\delta = 0.005$ (with $h = 1/128$, $k = 0.00002$).

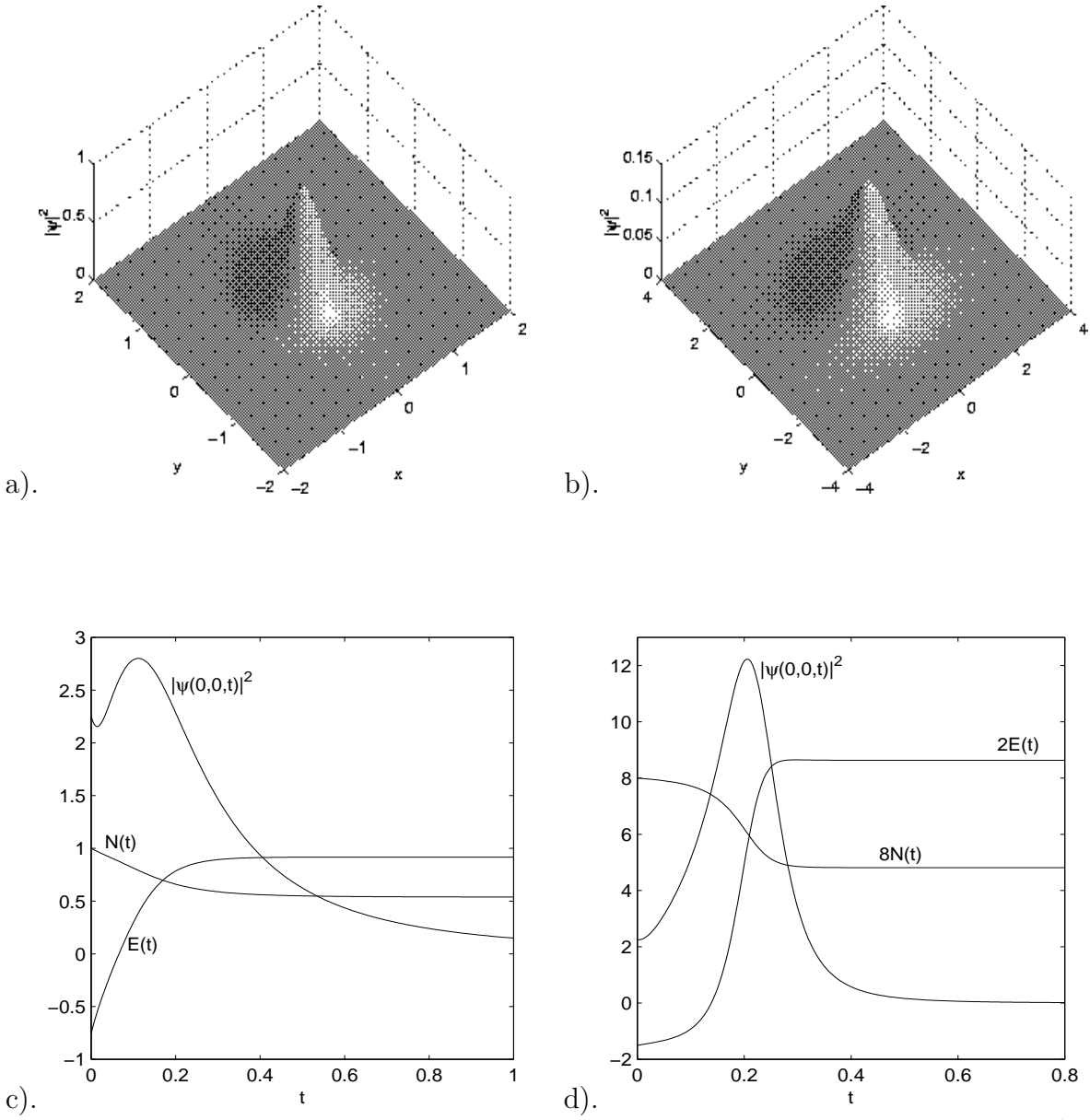


Figure 3: Numerical results in Example 1 case III. Surface plot of the density $|\psi|^2$ with $\delta = 0.01$: a). At time $t = 0.4$, b). $t = 1.0$. Normalization, energy and central density $|\psi(0,0,t)|^2$ as functions of time: c). with $\delta = 0.01$, d). $\delta = 0.001$.

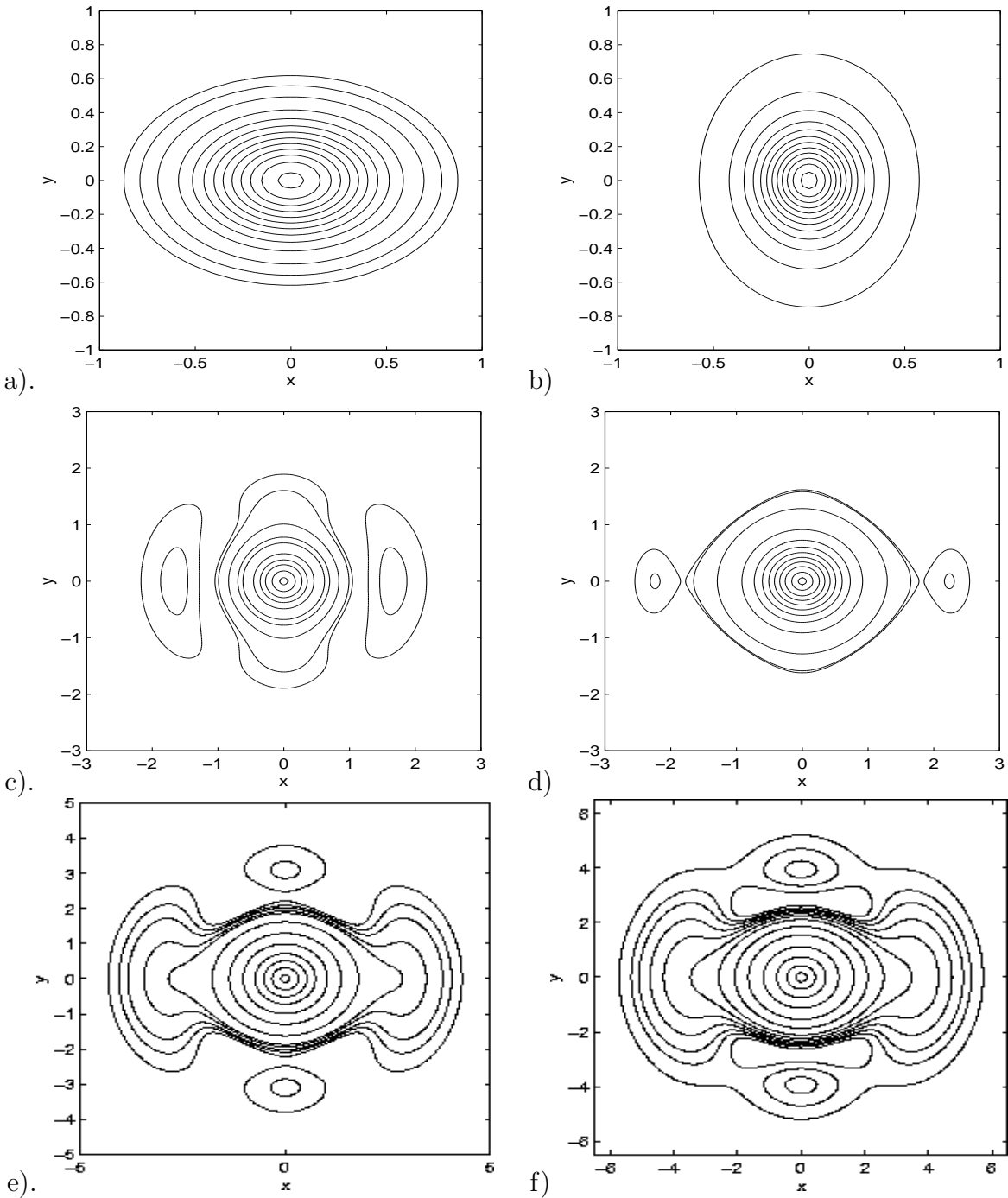


Figure 4: Contour plots of the density $|\psi|^2$ at different times in Example 1 case III with $\delta = 0.01$. a). $t = 0$, b). $t = 0.2$, c). $t = 0.4$, d). $t = 0.6$, e). $t = 0.8$, f). $t = 1$.

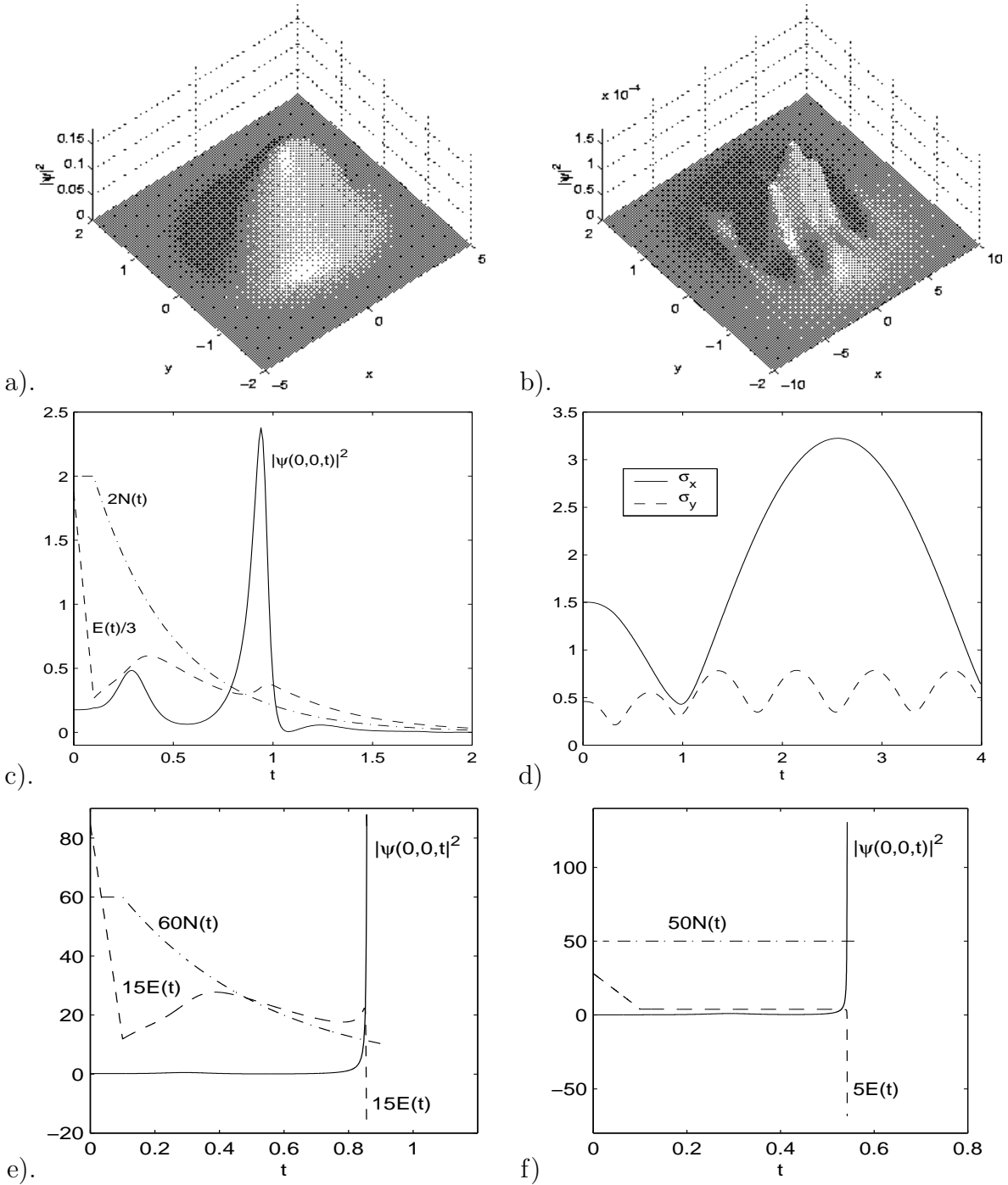


Figure 5: Numerical results in Example 2 case I. Surface plot of the density $|\psi|^2$ with $\delta = 1.25$: a). At time $t = 0$ (ground-state solution), b). $t = 2.8$. Normalization, energy and central density $|\psi(0,0,t)|^2$ as functions of time: c). with $\delta = 1.25$, e). $\delta = 1.1$, f). $\delta = 0$ (no damping). d). Condensate widths with $\delta = 1.25$.

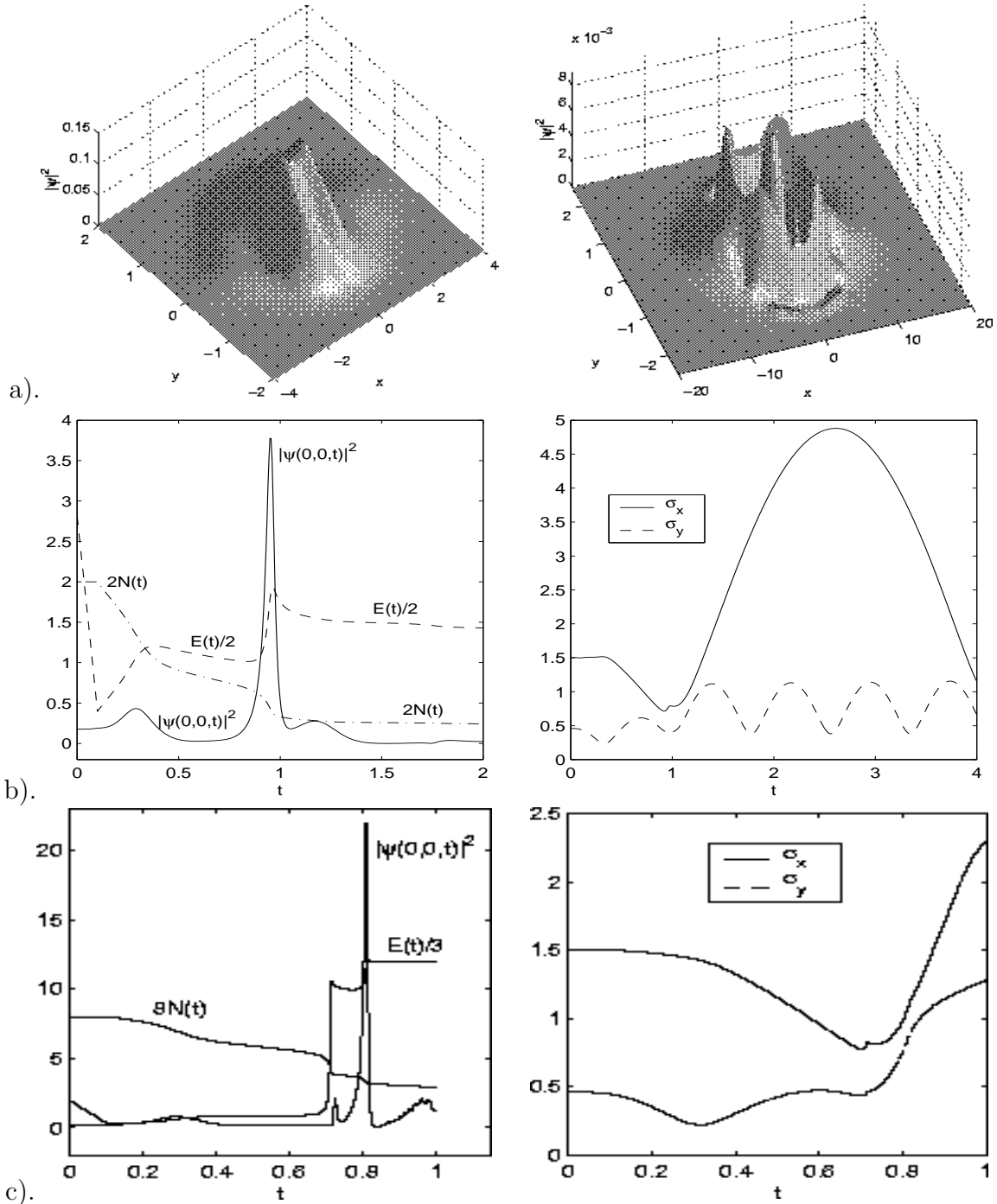


Figure 6: Numerical results in Example 2 case II. a). Surface plot of the density $|\psi|^2$ with $\delta = 0.15$: At time $t = 0.8$ (left column) and $t = 2.4$ (right column). Normalization, energy and central density $|\psi(0,0,t)|^2$ (left column) and condensate widths (right column) as functions of time: b). With $\delta = 0.15$; c). $\delta = 0.04$ (with .

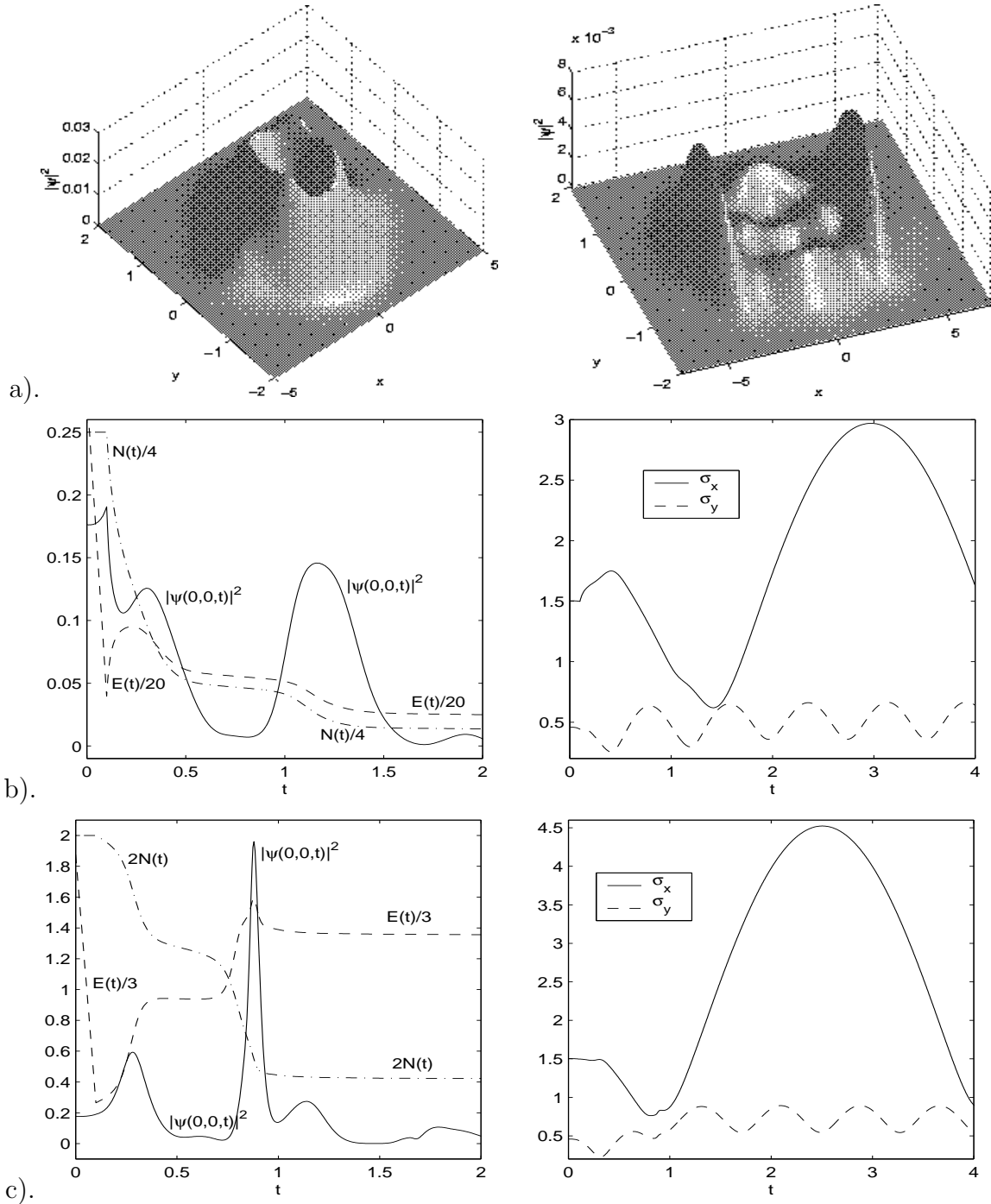


Figure 7: Numerical results in Example 2 case III. a). Surface plot of the density $|\psi|^2$ with $\delta = 0.15$: At time $t = 0.8$ (left column) and $t = 3.2$ (right column). Normalization, energy and central density $|\psi(0,0,t)|^2$ (left column) and condensate widths (right column) as functions of time: b). With $\delta = 0.15$; c). $\delta = 0.005$.

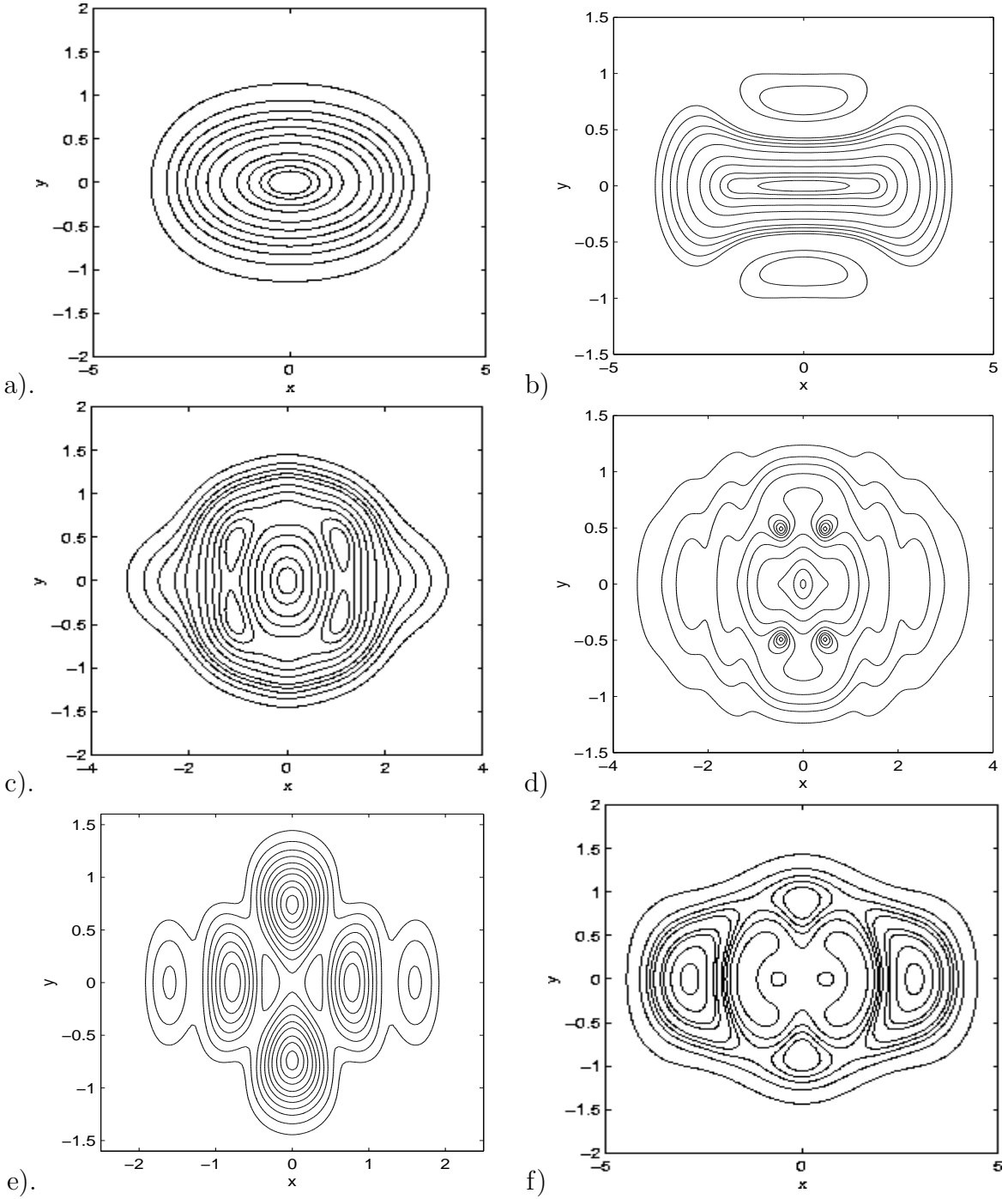


Figure 8: Contour plots of the density $|\psi|^2$ at different times in Example 2 case III with $\delta = 0.15$. a). $t = 0$, b). $t = 0.4$, c). $t = 0.8$, d). $t = 1.2$, e). $t = 1.6$, f). $t = 2.4$.